Technical University of Denmark

DTU

Designing finite-height two-dimensional photonic crystal waveguides

Søndergaard, Thomas; Bjarklev, Anders Overgaard; Kristensen, Martin; Østergaard, John Erland; Broeng, Jes

DTU Library
Technical Information Center of Denmark

Designing finite-height two-dimensional photonic crystal waveguides

T. Søndergaard,[a] A. Bjarklev, M. Kristensen, J. Erland, and J. Broeng
Research Center COM, Technical University of Denmark, Building 345, DK-2800 Lyngby, Denmark

Guidelines for designing planar waveguides based on introducing line-defects in two-dimensional photonic-crystal slabs are obtained by comparing calculations on two-dimensional structures with dispersion relations for the media above and below the slab. © *2000 American Institute of Physics.* [S0003-6951(00)04032-8]

Photonic crystals represent a promising class of periodic microstructured dielectric materials for the design of compact optical devices.[1–3] These materials are characterized by frequency intervals, photonic band gaps, where propagation of light in one or more dimensions is not allowed. Creating point-defects and line-defects in these crystals may lead to novel microcavities and waveguides.[3–12] Numerical calculations have shown that transmission coefficients above 98% for a 90° bend are possible for a crystal waveguide based on a large air line defect.[7]

Design parameters for photonic crystals that result in large photonic band gaps may be found in the literature (see for example Refs. 2, 13, and 14), and for some structures, band gaps exist at small wavelengths relative to the crystal lattice constant. This makes fabrication of structures with band gaps at a given wavelength an easier task. In this letter, however, we will show that the use of such band gaps is not promising for the design of finite-height photonic crystal waveguides. In particular, the high losses observed in Ref. 15 might be explained as a consequence of using a too short wavelength.

The existing literature on modeling of two-dimensional photonic crystals focuses on systems with dielectric pillars of infinite height and/or infinitely deep holes in a dielectric substrate.[4,6–8] For the case of two-dimensional photonic crystal slabs in air (finite height crystals), the existence of bound states has been demonstrated theoretically,[16,17] and experimental letters on crystal slabs have also appeared.[9,15,18] Naturally, planar waveguides based on photonic crystals cannot be of infinite height, and guidelines for the design of finite-height waveguides are, therefore, important for the realization of planar photonic crystal waveguides. In this letter, we compare calculations on two-dimensional photonic crystals with the dispersion relations for the media above and below the crystal slab. This type of comparison provides guidelines for which waveguide slabs may support guided modes for a given media above and below the slab.

Figure 1 shows two possible orientations of line-defects (waveguides) in a two-dimensional photonic crystal with dielectric pillars (dielectric constant ε_r) arranged on a triangular lattice in a dielectric background (dielectric constant ε_b). The width of the waveguide is denoted W, D is the diameter of the circular pillars, and Λ is the crystal lattice constant.

Consider the case of a waveguide (first orientation)

based on silicon pillars ($\varepsilon_r = 12$) in air ($\varepsilon_b = 1$). A suitable choice of pillar diameter is $D = 0.4\,\Lambda$ (see Ref. 2) yielding a large in-plane band gap for TM-polarized modes [(TM) transverse magnetic—refers to modes with the electric field along the z axis].

The electric field $\mathbf{E}$ of in-plane electromagnetic modes of the waveguide may be written on the form

$$\mathbf{E}_k(x,y) = \mathbf{U}_k(x,y)e^{ikx}, \tag{1}$$

where k is a Bloch wave number, x, y are spatial coordinates (as defined in Fig. 1), $i = \sqrt{-1}$, and $\mathbf{U}$ is a Bloch function satisfying $\mathbf{U}_k(x,y) = \mathbf{U}_k(x+\Lambda,y)$. The in-plane TM-band diagram for the infinite height pillar waveguide is shown for two waveguide widths W in Fig. 2. The diagram was calculated using plane-wave-expansion theory and a variational principle.[19] The gray regions represent a continuum of allowed frequencies Λ/λ, where λ is the free-space wavelength, as a function of k. These modes are allowed to propagate in the crystal structure surrounding the waveguide and are not guided modes. However, the discrete bands seen in Fig. 2 represent modes that are localized to the waveguide.

Consider the same arrangement of pillars, where these pillars are now finite height pillars on a substrate with the same refractive index as the pillars. The material above the pillars is assumed to be air. The air-dispersion relation is shown in Fig. 2 as the air line. All combinations of $(k,\Lambda/\lambda)$ above this line are allowed in free space. Indeed, for the infinite-height waveguide with $W = 0.3\,\Lambda$ there are guided modes with $(k,\Lambda/\lambda)$ that are not allowed in free space. The corresponding dispersion line for the substrate material is

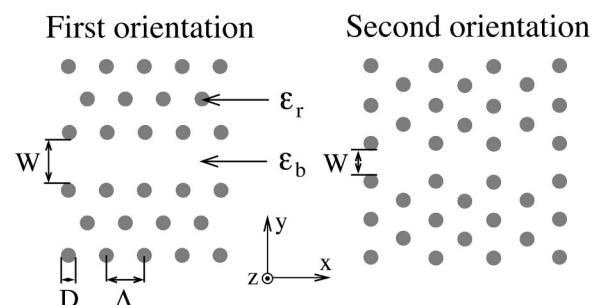FIG. 1. Two-dimensional photonic crystal waveguide created by introducing a line defect in a photonic crystal with dielectric rods (dielectric constant ε_r) arranged on a triangular lattice in a dielectric background (dielectric constant ε_b). First and second orientation denotes two possible symmetry directions in the crystal for the line defect.
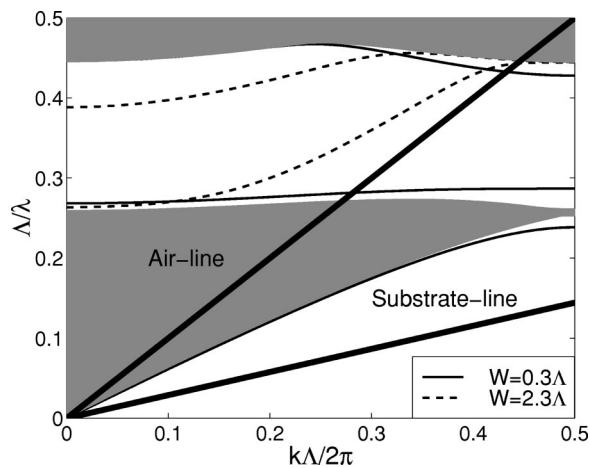
[a]Electronic mail: ts@com.dtu.dk

FIG. 2. TM-band diagram for a photonic crystal waveguide (first orientation) created by introducing a line defect in a two-dimensional photonic crystal with dielectric silicon rods arranged on a triangular lattice. Defect bands are shown for two waveguide widths $W = 0.3$ and $2.3\ \Lambda$, where Λ is the crystal lattice constant.

FIG. 3. TE-band diagram for a photonic crystal waveguide created by introducing a line defect (first orientation) in a two-dimensional crystal with holes arranged on a triangular lattice in silicon.

shown as the substrate line, and we note that all allowed combinations of $(k, \Lambda/\lambda)$ for the infinite height crystal are also allowed in the high-index substrate. Consequently, the finite height waveguide may suffer from severe losses due to scattering of light into the substrate. For the narrow width waveguide these losses might be overcome by choosing a low-index substrate. However, for waveguides with large W (the case of $W = 2.3\ \Lambda$ is shown in Fig. 2), where light is restricted to an air line defect, the $(k, \Lambda/\lambda)$ of the discrete bands tend to stay above the air line. Therefore, even though the case of pillars and light propagating in an air line defect (large W) is interesting from a physical point of view (the in-plane guidance mechanism is not total internal reflection), the simplest of such finite-height waveguides will not only suffer from severe losses due to scattering into the substrate but also from losses due to scattering into the air region above the photonic crystal slab. Band diagrams for waveguides based on creating a wide air line defect in photonic crystals with rods arranged on a square lattice may be found in Ref. 8, and by including the air line in these diagrams a similar conclusion is reached.

Note that for finite-height crystals the band gap for TE/TM polarization [(TE) transverse electric—refers to modes with the magnetic field along the z axis] is transformed into a band gap for odd and even modes, and the height of the crystal slab is also an important design parameter.[16] Determination of the optimum height for the crystal slabs requires full three-dimensional calculations as in Refs. 16 and 17.

A more promising choice of structure for finite-height planar photonic crystal waveguides is the case of holes ($\varepsilon_r = 1$) in a high-index material ($\varepsilon_b = 12$). Here, we will choose a hole diameter $D = 0.81\ \Lambda$, where the crystal exhibits a reasonable TE band gap. A TE-band diagram for first line-defect orientation for the infinitely deep hole waveguide is shown in Fig. 3 for the waveguide widths $W = 0.25$ and $0.75\ \Lambda$. The small width $W = 0.25\ \Lambda$ was chosen to illustrate a situation with a limited number of defect bands. As the width increases to $W = 0.75\ \Lambda$ the number of defect bands in the band gap increases, and the bands are also shifted in
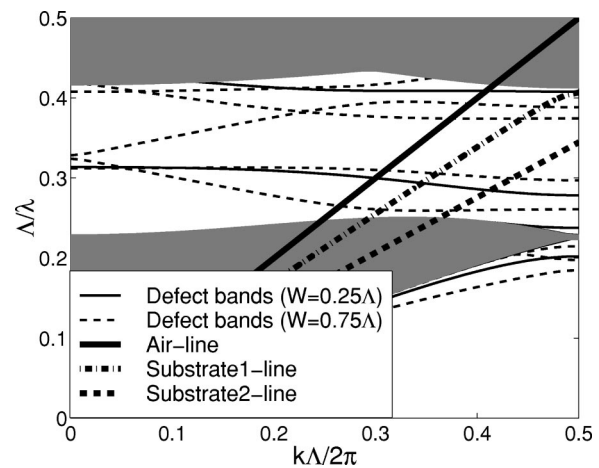
frequency. Indeed for the discrete bands there are electromagnetic modes with $(k, \Lambda/\lambda)$ below the air line, and photonic crystal waveguide slabs (as the one reported in Ref. 9) with air above and below the slab may support guided modes.

A design, where the material below the slab is not air, may be more convenient from a fabrication point of view. The substrate1 line in Fig. 3 represents the lowest allowed frequency for a given k in a silica photonic-crystal substrate (first orientation, $\varepsilon_r = 1$, $\varepsilon_b = 2.1$, $D = 0.81\ \Lambda$, $W = 0.25\ \Lambda$). In this case the holes penetrate from the silicon photonic crystal slab deep into the silica substrate. Indeed for the discrete bands there are also modes with $(k, \Lambda/\lambda)$ below the substrate1 line. Choosing a substrate based on homogeneous silica results in the substrate2 line. Clearly, for the silica photonic-crystal substrate (substrate 1), a larger range of frequencies may be supported by the waveguide. For the silica substrate (substrate 2) frequencies $\Lambda/\lambda > 0.345$ are above the substrate2 line. If larger D/Λ are chosen, the band gap moves up in frequency, and complete band gaps (for both TE and TM polarization) may exist. In Ref. 15, measurements were carried out for this type of waveguide (substrate 2 below the slab and air above) using normalized frequencies $\Lambda/\lambda > 0.5$, and high losses were observed. High losses are in agreement with the fact that frequencies $\Lambda/\lambda > 0.5$ are above the air line (and certainly above the substrate2 line).

A TE-band diagram for the case of second line-defect orientation for the infinitely deep hole waveguide ($\varepsilon_r = 1$, $\varepsilon_b = 12$, $D = 0.81\ \Lambda$, $W = 0.2\ \Lambda$) is shown in Fig. 4. The important observation in this case is that since the crystal periodicity for second orientation is larger than for first orientation the available k space is consequently smaller. In this case frequencies $\Lambda/\lambda > 0.29$ are above the air line, and the limited available k space severely restricts the useful range of frequencies.

In conclusion, photonic crystal waveguides based on creating a large air line-defect in a periodic arrangement of dielectric silicon pillars does not support bound modes with combinations of wave vectors and frequencies below the air line. However, guided modes may be possible when high-index defects are introduced. Photonic crystal slabs based on
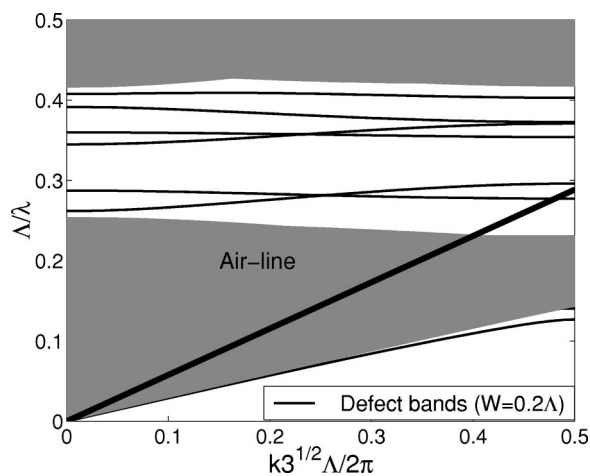
FIG. 4. TE-band diagram for a photonic crystal waveguide created by introducing a line defect (second orientation) in a two-dimensional crystal with holes arranged on a triangular lattice in silicon.

holes in a silicon slab with air above and below the slab does allow modes with wave vectors and frequencies below the air line. As a material above and below the silicon photonic crystal slab, homogeneous silica and silica photonic crystals may also be used. In this case, silica photonic crystals results in the largest useful range of frequencies. Line defects introduced along directions with large periodicity results in a severely limited useful range of frequencies. Determination of the optimum height of crystal waveguide slabs requires full three-dimensional calculations.

[1] E. Yablonovitch, Phys. Rev. Lett. **58**, 2059 (1987).
[2] J. D. Joannopoulos, R. D. Meade, and J. N. Winn, *Photonic Crystals* (Princeton University Press, Princeton, NJ, 1995).
[3] P. R. Villeneuve, S. Fan, and J. D. Joannopoulos, Phys. Rev. B **54**, 7837 (1996).
[4] J. B. Nielsen, T. Søndergaard, S. E. Barkou, A. Bjarklev, and J. Broeng, IEEE Photonics Technol. Lett. **12**, 60 (2000).
[5] T. Søndergaard and K. H. Dridi, Phys. Rev. B **61**, 15688 (2000).
[6] H. Benisty, J. Appl. Phys. **79**, 7483 (1996).
[7] A. Mekis, J. C. Chen, I. Kurland, S. Fan, P. R. Villeneuve, and J. D. Joannopoulos, Phys. Rev. Lett. **77**, 3787 (1996).
[8] A. Mekis, S. Fan, and J. D. Joannopoulos, Phys. Rev. B **58**, 4809 (1998).
[9] M. D. B. Charlton, G. J. Parker, and M. E. Zoorob, J. Mater. Sci.: Mater. Electron. **10**, 429 (1999).
[10] O. Painter, R. K. Lee, A. Scherer, A. Yariv, J. D. O'Brien, P. D. Dapkus, and I. Kim, Science-AAAS-Weekly Paper Edition, **284**, 1819 (1999).
[11] E. Centeno, B. Guizal, and D. Felbacq, J. Opt. A: Pure Appl. Opt. **1**, L10 (1999).
[12] T. Søndergaard, IEEE J. Quantum Electron. **36**, 450 (2000).
[13] T. Søndergaard, J. Broeng, A. Bjarklev, K. Dridi, and S. E. Barkou, IEEE J. Quantum Electron. **34**, 2308 (1998).
[14] D. Cassagne, C. Jouanin, and D. Bertho, Phys. Rev. B **52**, R2217 (1995).
[15] M. Tokushima, H. Kosaka, A. Tomita, and H. Yamada, Appl. Phys. Lett. **76**, 952 (2000).
[16] S. G. Johnson, S. Fan, P. R. Villeneuve, and J. D. Joannopoulos, Phys. Rev. B **60**, 5751 (1999).
[17] S. Kuchinsky, D. C. Allan, N. F. Borelli, and J.-C. Cotteverte, Opt. Commun. **175**, 147 (2000).
[18] D. Labilloy, H. Benisty, C. Weisbuch, T. F. Krauss, R. M. De La Rue, V. Bardinal, R. Houdre, U. Oesterle, D. Cassagne, and C. Jouanin, Phys. Rev. Lett. **79**, 4147 (1997).
[19] R. D. Meade, A. M. Rappe, K. D. Brommer, J. D. Joannopoulos, and O. L. Alerhand, Phys. Rev. B **48**, 8434 (1993).